ROYAL SOCIETY OF CHEMISTRY

PAPER

White light emitting diodes with enhanced CCT uniformity and luminous flux using ZrO_2 nanoparticles

Kuo-Ju Chen,[a] Hau-Vei Han,[a] Hsin-Chu Chen,[a] Chien-Chung Lin,*[b] Shih-Hsuan Chien,[a] Chung-Ching Huang,[a] Teng-Ming Chen,[c] Min-Hsiung Shih[ad] and Hao-Chung Kuo*[a]

To enhance the uniformity of correlated color temperature (CCT) and luminous flux, we integrated ZrO_2 nanoparticles into white light-emitting diodes. This novel packaging scheme led to a more than 12% increase in luminous flux as compared to that in conventional dispensing structures. This was attributed to the scattering effect of ZrO_2 nanoparticles, which enhanced the utilization of blue light. Moreover, the CCT deviation was reduced from 522 to 7 K in a range of −70 to +70°, and essentially eliminated the yellow ring phenomenon. The haze measurement indicated strong scattering across the visible spectrum in the presence of ZrO_2 in the silicone layer, and this finding also substantiates our claim. In addition, the chromaticity coordinate shift was steady in the ZrO_2 dispensing package structure as the drive current increased, which is crucial for indoor lighting. Combined with its low cost, easy fabrication, and superior optical characteristics, ZrO_2 nanoparticles can be an effective performance enhancer for the future generation of white light-emitting devices.

Introduction

Recently, light-emitting diodes (LEDs) have been widely used as a solid-state lighting source due to their low cost, longer life, higher efficiency and environmental sustainability.[1–4] One of the very major applications of LEDs is their use as indoor lighting replacement for light bulbs. The most basic and common method for producing white light is combining blue LEDs with yellow phosphor ($Y_3Al_5O_{12}$:Ce^{3+}) in the package. Although this strategy is widely used in the industry, the primary disadvantage is a poor color rendering index (CRI).[5] Therefore, several methods have been pursued in the field addressing white LED technology. To enhance the CRI value of white LEDs, some advanced red phosphor technologies have been reported.[6,7] Moreover, the use of multiple lateral quantum wells (QWs) and various facets have resulted in multiple emission spectra and obtained white LEDs.[8,9] Furthermore, recent studies have also used various methods such as large overlap

QWs[10–13] and the surface plasmon approach[14,15] for suppressing the charge separation problem in InGaN QWs to improve the IQE in green/yellow/red spectral regimes, which are imperative for tricolor white LEDs with only InGaN QWs.

In many cases, a freely dispensed method has been adapted for easy implementation and low cost, but its luminous efficiency and uniformity of correlated color temperature (CCT) still require improvement.[16] Increasing the amount of received photons passing through these layers of packages is crucial for the luminous efficiency of an LED. In the past, there have been numerous methods for enhancing light extraction. The dual-layer graded-refractive index (RI) encapsulant was used to enhance light extraction.[17] Luo *et al.* employed the phosphor-on-top packaging configuration to enhance the phosphor efficiency.[18] In another attempt to use a remote phosphor design,[19] the great separation between the blue LEDs and phosphor was used to prevent backscattering of the phosphor.

In addition to lumen efficiency, color uniformity is one of the major problems in white LED fabrication. According to a previous study, the problem is associated with the different ratios of blue and yellow emissions, which results in different CCTs at various angles.[19] In white LEDs, one of the direct consequences of nonuniform CCTs is called a yellow ring phenomenon, and it becomes critical when the device package used is large or sophisticated; thus, this problem must be solved. Kuo *et al.* used the remote phosphor structure pattern to ameliorate CCT deviation.[20] A conformal-phosphor structure was also proposed to reduce angular CCT deviations.[21] Other

[a] Department of Photonics & Institute of Electro-Optical Engineering, National Chiao Tung University, Hsinchu 30010, Taiwan. E-mail: hckuo@faculty.nctu.edu.tw; Fax: +886-3-5735601; Tel: +886-3-5712121#56304

[b] Institute of Photonic System, National Chiao Tung University, Tainan 711, Taiwan. E-mail: chienchunglin@faculty.nctu.edu.tw; Fax: +886-6-3032535; Tel: +886-6-3032121#57754

[c] Phosphors Research Laboratory, Department of Applied Chemistry, National Chiao Tung University, Hsinchu 30010, Taiwan

[d] Research Center for Applied Sciences, Academia Sinica, 128 Academia Rd., Sec. 2 Nankang, Taipei 115, Taiwan

methods, such as improved silicon lens design[22] and modification of the shape of the surface phosphor layer[23] were proposed and demonstrated. Moreover, some researches demonstrate the uniform angular CCT for white LED by the optimized design package and using with patterned sapphire substrate.[24,25] Furthermore, the graded-refractive-index multi-layer encapsulation structure was also demonstrated by incorporating nanoparticles into the packaging materials.[26] The scattering effect of nanoparticles could strongly influence the optical path and change the CCT deviation in white LEDs.[27] However, the luminous flux of this structure must still be enhanced. Therefore, simultaneously achieving high luminous efficiency and excellent light quality is a critical factor that could help white LEDs become the primary solid-state lighting source in the market.

In this study, ZrO_2 nanoparticles were employed to enhance the luminous efficiency and light quality of LEDs. By codoping the ZrO_2 nanoparticles with the phosphors, the enhancement of the light scattering effect enabled the improved utilization of blue light, resulting in an increased luminous flux. Simultaneously, the presence of ZrO_2 nanoparticles also provided a scattering capability that reduced angle-dependent CCT deviations.

Experiment

The dispensing method was modified to incorporate ZrO_2 nanoparticles (Moretech Precision Technology) into white LEDs. Fig. 1(a) and (b) illustrates the schematic diagrams of a ZrO_2-doped device and a conventional device. The experimental flow was as follows: First, a GaN-based blue chip with an emission wavelength of 450 nm was bonded in the lead-frame package. Second, the ZrO_2 nanoparticles were uniformly mixed with the YAG phosphor (Intematix) and the silicone encapsulant was dispensed in the package. In the reference samples, only the phosphors were uniformly mixed with the silicone

encapsulant. The YAG phosphor powder shows that the full width at half maximum of emission was approximately 100 nm. The output power of the selected blue LED chips was 120 mW at a driving current of 120 mA. To investigate the influence of the ZrO_2 nanoparticles on the improvement of the CCT and luminous flux of a package, different weight percentages of the ZrO_2 were added to the phosphor and silicone encapsulant. Fig. 1(c) shows the cross-sectional view of the scanning electron microscopy (SEM) image of the ZrO_2 nanoparticles in the silicone encapsulant. The particle sizes of the YAG and ZrO_2 nanoparticles were approximately 10 μm and 300 nm, respectively.

Results and discussion

Shown in Fig. 2(a) are the luminous fluxes of the white LEDs in the packages with different contents of ZrO_2 nanoparticles measured at 120 mA. The phosphor concentrations of the conventional structure and ZrO_2 nanoparticle (1 wt%) dispensing structure are the same, but the lumen output of the ZrO_2 nanoparticle dispensing structure was 12% higher than that of the conventional structure. The nanoparticle-embedded device had a higher yellow ray intensity than the conventional device because of the improved conversion ratio from blue photons, resulting in a higher luminous efficiency. The scattering effect of the ZrO_2 nanoparticles enhanced the efficiency because the prolonged optical path of the blue light caused by scattering led to the higher possibility of exciting the yellow phosphor; thus increasing yellow photon generation. However,
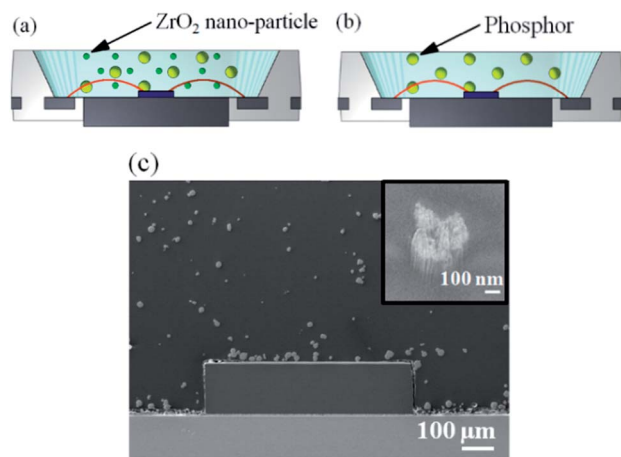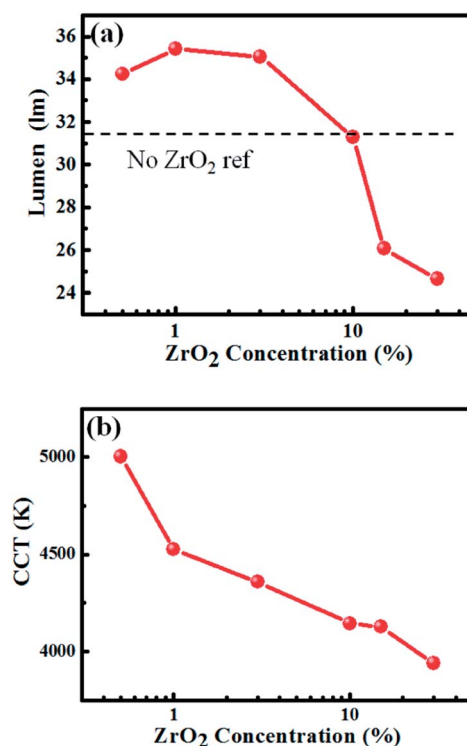

Fig. 1 Schematic cross-sectional view of (a) nanoparticle dispense (b) conventional dispense phosphor structure (c) SEM images of cross section of nanoparticle dispense structure and the inset shows the SEM images of ZrO_2 nanoparticle.

Fig. 2 (a) The lumen flux and (b) correlated color temperature with the different concentration of ZrO_2 nanoparticle.

as the concentration of the ZrO_2 nanoparticles becomes larger, the transmittance of the ZrO_2 layer would be lower, as shown in Fig. 1. Therefore, LED device with high concentration ZrO_2 nanoparticle leads to eventual lower lumen efficiency due to the light trapping and absorption phenomenon between the phosphor materials.[19] Fig. 2(b) shows the CCTs with the different concentrations of ZrO_2 nanoparticles. The CCT of the no-ZrO_2 reference sample was 5319 K, and it dropped from this value as the concentration of ZrO_2 increased because of the higher yellow conversion ratio.

The luminous flux and the luminous efficiency measured using a calibrated integrating sphere are plotted in Fig. 3(a) as a function of injection currents ranging from 50 to 500 mA. Regarding luminous flux, the optimized concentration of ZrO_2 nanoparticles is 1 wt% and its luminous flux exceeded that of conventional devices over the entire current range. Measured at a 120 mA current injection, the emission spectra of the reference and ZrO_2-doped devices are shown in Fig. 3(b). The scattering effect of the ZrO_2 nanoparticles in the encapsulant resin prevented the original Lambertian blue ray from escaping the resin directly, which increased the possibility to excite the yellow phosphor. Therefore, the increased utilization rate of the blue ray increased the output of the yellow light, resulting in the enhancement of lumen efficiency.

To understand the influence of the scattering effect on the variations of the CCT and luminous flux, the angle-dependent CCTs of LED packages containing different amounts of ZrO_2

nanoparticles were investigated and shown in Fig. 4(a). The uniformity of the angle-dependent CCTs was greatly improved when the devices were doped with ZrO_2 nanoparticles. This observation indicates that increasing the ZrO_2 nanoparticle concentration of the dopant yielded a stronger scattering effect. In general, the uniformity of CCTs is defined as the maximum CCT minus the minimum CCT. Without doping with ZrO_2 nanoparticles, the reference CCT was located at a high level (approximately 5319 K), and a higher CCT implied a higher extraction of blue light, which caused higher CCT deviation. When the devices were doped with ZrO_2 nanoparticles, the CCT difference observed at 0° and 70° was essentially eliminated. The inset picture in Fig. 4(a) shows the far-field images of uniform white light generated from a ZrO_2 nanoparticle-doped LED. Fig. 4(b) shows the figure of merit (FOM), which was defined as

$$FOM = \frac{Lumen_{ZrO_2} - Lumen_{No\ ZrO_2}}{\Delta CCT} \qquad (1)$$

It was discovered that the CCT deviation dropped rapidly from 522 K (reference) to 57 K (3 wt% ZrO_2 doping), and then to 7 K (10 wt% ZrO_2 doping). Using high ZrO_2-doping rates resulted in uniform CCT angular distributions; however, it also
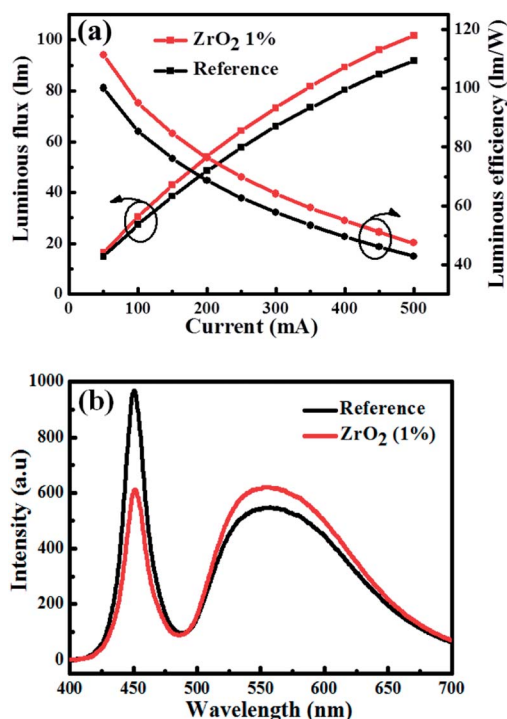

Fig. 3 (a) Luminous flux and the luminous efficiency of nano-particle dispense and the conventional dispense phosphor structure driven at the current from 50 to 500 mA (b) the emission spectra of nano-particle dispense and the conventional remote phosphor structure at 120 mA.
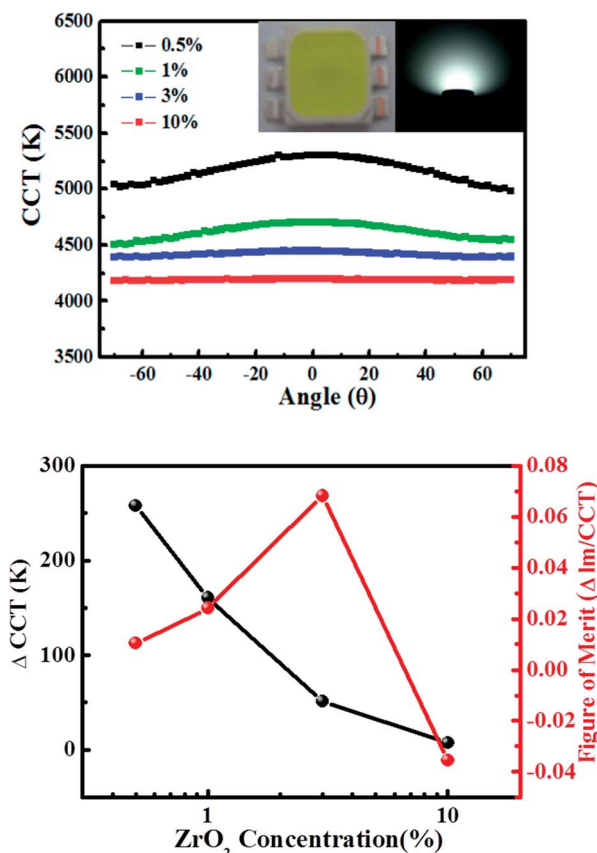

Fig. 4 (a) The angular-dependent correlated color temperature of ZrO_2 nano-particles dispense phosphor structure and (b) the CCT deviation and the figure of merit of different concentrations of ZrO_2 nano-particles in dispensed phosphor structure.

resulted in lumen reduction, as shown in Fig. 2(a). According to our definition of FOM, the optimal ZrO₂ doping concentration was discovered to be at 3%.

The effect of ZrO₂ doping on the phosphor and silicone was strong for the performance of the packaged device. The optical properties of ZrO₂-doped films, however, remained unclear. To probe further, a series of thin-film experiments, including transmission–absorption and haze, were performed to characterize this ZrO₂–phosphor–silicone mixture. Compared with that of the conventional dispensing structure, the absorption percentage in the ZrO₂ nanoparticle dispensing structure was discovered to increase from approximately 32% to nearly 42% at the wavelength of 460 nm. This improvement led to the generation of a higher portion of yellow light in the ZrO₂-doped samples; thus, luminous efficiency was increased.

In addition, haze measurement was employed to investigate the scattering effect of ZrO₂ nanoparticles with the phosphor layer, and the haze intensity was defined as[28]

$$\text{Haze intensity} = T_{\text{diffraction}}/T_{\text{total}} \times 100\% \qquad (2)$$

where $T_{\text{diffraction}}$ was the diffractive transmittance (excluding the 0-order diffraction), and T_{total} was the total transmittance. Fig. 5(b) shows the haze intensities at various ZrO₂ doping concentrations in the phosphor layer. The measured haze intensity was observed to increase from 45% to 94% at a wavelength of 460 nm after doping with ZrO₂ nanoparticles. When more ZrO₂ nanoparticles were used in the dopants, the

Fig. 5 (a) Absorption and (b) the haze intensity of the different concentration of ZrO₂ nano-particle.

haze intensity became stronger; it increased to 100% when the dopant used had 10 wt% ZrO₂ nanoparticles. From the perspective of haze measurement, we could certainly see higher scattering effect by larger ZrO₂ particles. However, there is a limitation on the actual size of ZrO₂ nano-particles when the output lumen and CCT are both considered as important characteristics of a LED. From previous research,[29,30] a rising extinction coefficient can be seen in the 0–1mm range. A higher extinction coefficient means stronger re-absorption of photons due to back-scattering, and thus not very favorable for enhancement of LED performance. From our own experiment, as shown in Fig. 2(a), when the concentration of ZrO₂ is up, the output lumen is not always increasing but dropping after 10%. The effective volume of ZrO₂ particles increases as we mixed more, so this figure can be treated as an indirect proof of the limitation on the particle size.

In this study, after doping the ZrO₂ nanoparticle in the phosphor layer, the effective index will be changed with the different ZrO₂ nanoparticle concentration. Moreover, the refractive indices (RI) of silicone, phosphor, ZrO₂ nanoparticle are 1.4, 1.8 and 2.23, which are obtained from the ref. 31 Thus, the RI of the phosphor layer with ZrO₂ nanoparticle is calculated using the following equation[32]

$$RI = V_1 RI_1 + V_2 RI_2 + V_3 RI_3,$$

where V_1, V_2 and V_3 are the concentrations of the materials, which is calculated in the weight ratio of the materials. For the ZrO₂ nanoparticle dispensing structure, the mixing ratio of the ZrO₂ nanoparticles to phosphor layer in the dispensing structure were 1 wt% and 3 wt%, respectively. Therefore, the RIs of the phosphor layer in each layer were 1.428 and 1.445. To discuss the influence of the different refractive index layers, a TFCalc32 simulation was used.[33] Compared with the conventional dispense structure, the light extraction for ZrO₂ nanoparticle dispensing structure is almost the same due to the nearly identical refractive index. Thus, the enhancement of lumen flux for ZrO₂ nanoparticle dispensing structure might be attributed solely to the scattering effect of the ZrO₂ nanoparticle.

To numerically evaluate the scattering effect of the ZrO₂ nanoparticles, a Mie-scattering simulation was performed to analyze the scattering effect of the different ZrO₂ dopant concentrations.[34–36] In our model, there were no phosphors and only ZrO₂ nanoparticles were present in the medium to reduce the complexity of the model. The RI of the ZrO₂ nanoparticle with silicone was 2.23 at the wavelength of 460 nm. The particle size of ZrO₂ was approximately 300 nm and the dopant content of ZrO₂ nanoparticles was approximately 1% and 3%, respectively, as represented in Fig. 6(a) and (b). The haze intensity of the simulated device structure with lower ZrO₂ dopant content showed almost 100% prior to reaching 500 nm and decreased slowly when the wavelength was longer than 500 nm. According to the simulated results, the scattering effect of ZrO₂ corresponds with our experimental results. When doping with a higher content of ZrO₂, the haze intensity was nearly the same as that for the wavelength ranging from 300 to 700 nm.
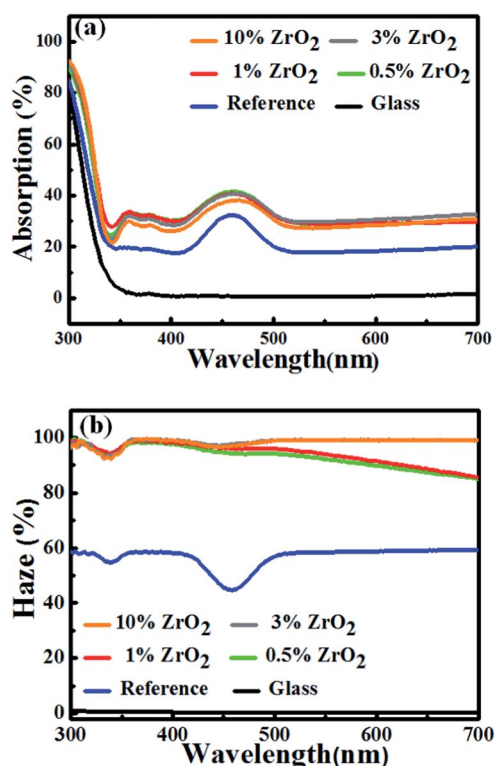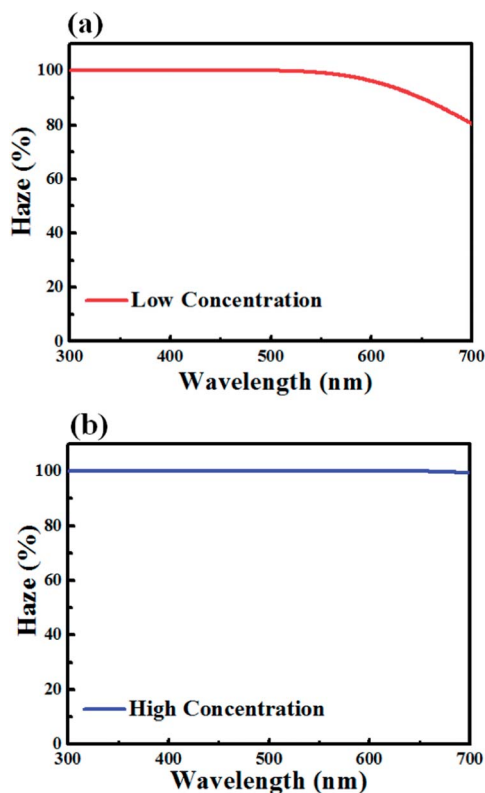
Fig. 6 The simulated results of haze intensity in the concentration of (a) 1% and (b)3%.

Finally, the color quality of ZrO_2-doped devices must be evaluated. One of the widely adapted standards is to measure its chromaticity coordinates under normal operations. The chromaticity coordinates of the dispensing structure with different contents of ZrO_2 dopant at 120 mA are shown in Fig. 7(a). As the ZrO_2-nanoparticle content increased, the chromaticity coordinates gradually shifted to the yellow region, and this observation indicated that the intensity of yellow light became stronger and finally led to lower CCTs. Fig. 7(b) illustrates the detailed shifting of chromaticity coordinates with different contents of ZrO_2-nanoparticle dopants at current injections of 50 to 500 mA. Although it is not obvious, the chromaticity coordinates show slighter shifting in the ZrO_2 dispensing package structure compared with the conventional structure with increasing driving current, which can be attributed to the scattering effect of ZrO_2 nanoparticles. The maximum color deviation value of the structure with ZrO_2 nanoparticles was 0.006, indicating superior CCT stability with the increasing driving current. The angular dependence of the emission intensity was also examined to investigate the performance of package structures with different contents of ZrO_2-nanoparticle dopants and that of the conventional dispensing structure, as shown in Fig. 7(c). The far-field emission pattern of our ZrO_2-doped LEDs also showed the characteristics of a Lambertian source, as shown in Fig. 7(d). With these properties combined, this type of ZrO_2 nanoparticle-modified LED can exhibit superior performance under various driving current densities and generate high-quality white light.
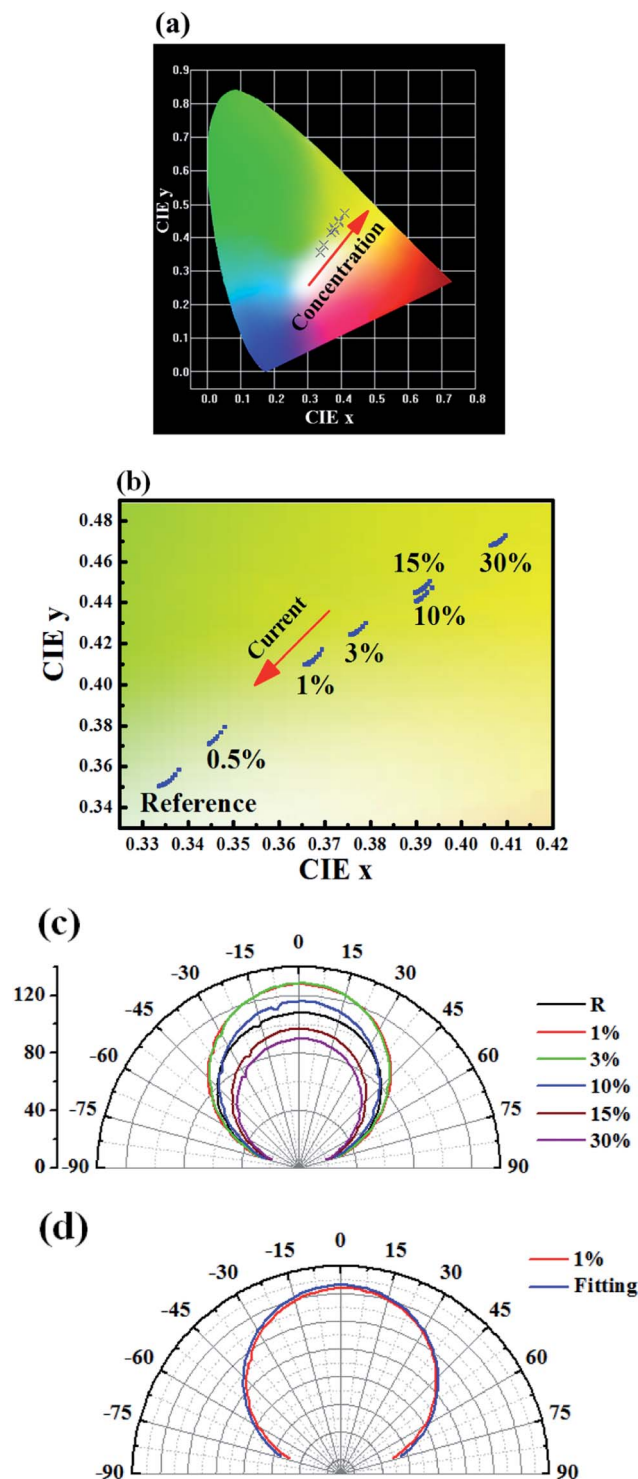

Fig. 7 Chromaticity coordinate of LED (a) with different concentration of ZrO_2 nano particle (b) with different current from 50 to 500 mA (c) the relative lumen with different concentration of ZrO_2 nano-particle (d) 1% and fitting line at different incident from −90° to 90°.

Conclusion

In conclusion, the effect of ZrO_2-nanoparticle doping in the package was investigated for improving white LEDs. It was

revealed that this novel packaging method leads to at least a 12% higher lumen than that of conventional structures at 1 wt% ZrO_2 concentration. This improvement is due to the scattering effect of ZrO_2 nanoparticles and the enhanced utilization of blue light. Moreover, the deviation of the CCT is also reduced from 522 K (reference) to 7 K (10 wt% ZrO_2 doping), and this result is comparable to that of a conventional diffuser plate; however, the ZrO_2-doped design does not sacrifice the output luminous efficiency. Based on the haze measurements, the haze intensity becomes stronger and increases to 100% as the amount of ZrO_2 nanoparticles used increases, which corresponds with the simulation results. The chromaticity coordinate shift is stable in the ZrO_2-dispensed package structure with the increasing drive current and the emission pattern is close to Lambertian. The doping of ZrO_2 nanoparticles to achieve highly uniform CCTs and high luminous efficiencies provides an appropriate solution for applications in solid-state lighting.

References

1 E. F. Schubert and J. K. Kim, *Science*, 2005, **308**, 1274–1278.
2 S. Nakamura, T. Mukai and M. Senoh, *Appl. Phys. Lett.*, 1994, **64**, 1687–1689.
3 S. Pimputkar, J. S. Speck, S. P. DenBaars and S. Nakamura, *Nat. Photonics*, 2009, **3**, 179–181.
4 K. J. Chen, B. C. Lin, H. C. Chen, M. H. Shih, C. H. Wang, H. T. Kuo, H. H. Tsai, M. Y. Kuo, S. H. Chien, P. T. Lee, C. C. Lin and H. C. Kuo, *IEEE Photonics J.*, 2013, **5**, 8200508.
5 K. J. Chen, H. C. Chen, M. H. Shih, C. H. Wang, M. Y. Kuo, Y. C. Yang, C. C. Lin and H. C. Kuo, *J. Lightwave Technol.*, 2012, **30**, 2256–2261.
6 S. E. Brinkley, N. Pfaff, K. A. Denault, Z. J. Zhang, H. T. Hintzen, R. Seshadri, S. Nakamura and S. P. DenBaars, *Appl. Phys. Lett.*, 2011, **99**, 241106.
7 Y. Zhang, L. Wu, M. Y. Ji, B. A. Wang, Y. F. Kong and J. J. Xu, *Opt. Mater. Express*, 2012, **2**, 92–102.
8 M. Funato, T. Kondou, K. Hayashi, S. Nishiura, M. Ueda, Y. Kawakami, Y. Narukawa and T. Mukai, *Appl. Phys. Express*, 2008, **1**, 011106.
9 I. K. Park, J. Y. Kim, M. K. Kwon, C. Y. Cho, J. H. Lim and S. J. Park, *Appl. Phys. Lett.*, 2008, **92**, 091110.
10 D. F. Feezell, J. S. Speck, S. P. DenBaars and S. Nakamura, *J. Disp. Technol.*, 2013, **9**, 190–198.

11 H. Zhao, G. Liu, J. Zhang, J. D. Poplawsky, V. Dierolf and N. Tansu, *Opt. Express*, 2011, **19**, A991–A1007.
12 H. Zhao, G. Liu and N. Tansu, *Appl. Phys. Lett.*, 2010, **97**, 131114.
13 J. Zhang and N. Tansu, *J. Appl. Phys.*, 2011, **110**, 113110.
14 H. Zhao, J. Zhang, G. Liu and N. Tansu, *Appl. Phys. Lett.*, 2011, **98**, 151115.
15 C. H. Lu, C. C. Lan, Y. L. Lai, Y. L. Li and C. P. Liu, *Adv. Funct. Mater.*, 2011, **21**, 4719–4723.
16 H. C. Chen, K. J. Chen, C. H. Wang, C. C. Lin, C. C. Yeh, H. H. Tsai, M. H. Shih, H. C. Kuo and T. C. Lu, *Nanoscale Res. Lett.*, 2012, **7**, 1–5.
17 M. Ma, F. W. Mont, X. Yan, J. Cho, E. F. Schubert, G. B. Kim and C. Sone, *Opt. Express*, 2011, **19**, A1135–A1140.
18 H. Luo, J. K. Kim, E. F. Schubert, J. Cho, C. Sone and Y. Park, *Appl. Phys. Lett.*, 2005, **86**, 243505.
19 H. C. Chen, K. J. Chen, C. C. Lin, C. H. Wang, H. V. Han, H. H. Tsai, H. T. Kuo, S. H. Chien, M. H. Shih and H. C. Kuo, *Nanotechnology*, 2012, **23**, 265201.
20 H. C. Kuo, C. W. Hung, H. C. Chen, K. J. Chen, C. H. Wang, C. W. Sher, C. C. Yeh, C. C. Lin, C. H. Chen and Y. J. Cheng, *Opt. Express*, 2011, **19**, A930–A936.
21 H. T. Huang, C. C. Tsai and Y. P. Huang, *Opt. Express*, 2010, **18**, A201.
22 K. Wang, D. Wu, F. Chen, Z. Liu, X. Luo and S. Liu, *Opt. Lett.*, 2010, **35**, 1860–1862.
23 Y. Shuai, N. T. Tran and F. G. Shi, *IEEE Photonics Technol. Lett.*, 2011, **23**, 137–139.
24 C. C. Sun, C. Y. Chen, C. C. Chen, C. Y. Chiu, Y. N. Peng, Y. H. Wang, T. H. Yang, T. Y. Chung and C. Y. Chung, *Opt. Express*, 2012, **20**, 6622–6630.
25 K. C. Huang, T. H. Lai and C. Y. Chen, *Appl. Opt.*, 2013, **52**, 7376–7381.
26 F. W. Mont, J. K. Kim, M. F. Schubert, E. F. Schubert and R. W. Siegel, *J. Appl. Phys.*, 2010, **107**, 083120.
27 J. P. You, N. T. Tran and F. G. Shi, *Opt. Express*, 2010, **18**, 5055–5060.
28 H. T. Chiu, C. Y. Chang, C. L. Chen, T. Y. Chiang and M. T. Guo, *J. Appl. Polym. Sci.*, 2011, **120**, 202–211.
29 Y. Shuai, N. T. Tran and F. G. Shi, *IEEE Photonics Technol. Lett.*, 2011, **23**, 552–554.
30 T. Nguyen The, Y. Jiun Pyng and F. G. Shi, *J. Lightwave Technol.*, 2009, **27**, 5145–5150.
31 K. J. Chen, H. V. Han, L. B. C. Lin, H. C. Chen, M. H. Shih, S. H. Chen, K. Y. Wang, H. H. Tsai, P. Yu, P. T. Lee, C. C. Lin and H. C. Kuo, *IEEE Electron Device Lett.*, 2013, **34**, 1280–1282.
32 Y. H. Won, H. S. Jang, K. W. Cho, Y. S. Song, D. Y. Leon and H. K. Kwon, *Opt. Lett.*, 2009, **34**, 1–3.
33 K. J. Chen, H. C. Chen, M. H. Shih, C. H. Wang, H. H. Tsai, S. H. Chien, C. C. Lin and H. C. Kuo, *J. Lightwave Technol.*, 2013, **31**, 1941–1945.
34 C. F. Bohren and D. R. Huffman, *Absorption and Scattering of Light by Small Particles*, Wiley, New York, 1983.
35 D. Toublanc, *Appl. Opt.*, 1996, **35**, 3270–3274.
36 Y. H. Won, H. S. Jang, K. W. Cho, Y. S. Song, D. Y. Leon and H. K. Kwon, *Opt. Lett.*, 2009, **34**, 1–3.